Journal of Catalysis **203,** 213–231 (2001)
doi:10.1006/jcat.2001.3325, available online at http://www.idealibrary.com on IDEAL®

Dimethyl Branching of Long *n*-Alkanes in the Range from Decane to Tetracosane on Pt/H–ZSM-22 Bifunctional Catalyst

Marion C. Claude, Gina Vanbutsele, and Johan A. Martens

Centrum voor Oppervlaktechemie en Katalyse, Departement Interfasechemie, K.U. Leuven, Kasteelpark Arenberg 23, B-3001 Leuven, Belgium

Received April 9, 2001; revised June 1, 2001; accepted June 27, 2001

Single long *n*-alkanes in the range *n*-C_{10} to *n*-C_{24} were hydroisomerized at 233°C in a fixed-bed down-flow vapor-phase reactor loaded with Pt/H–ZSM-22 zeolite catalyst. The multibranched isomer fractions obtained by skeletal isomerization of the different *n*-alkanes were analyzed in detail with GC-MS. The large majority of multibranched isomers were dimethyl branched. In the preferred isomers, the tertiary carbon atoms carrying the methyl branchings were separated by 3 up to 14 carbon atom positions. Further peculiarities were the preferential formation of isomers with symmetric methyl positions on the chain. Among this family of "symmetric" isomers, the formation of 2,$x-3$-dimethyl–C_{x-2} isomer was favored in conversions of *n*-C_x alkanes with x equal to or smaller than 17 and disfavored with longer molecules. In the family of 3,*n*-dimethyl–C_{x-2} isomers obtained from the longest alkanes studied (*n*-C_{20}, *n*-C_{22}, *n*-C_{24}), the preferred *n* positions were from 8 to 12 and from 14 to 18. In the 4,*n*-dimethyl–C_{x-2} isomers, the preferred *n* positions were from 8 to 17. It was also found that the formation of a dimethyl-branched isomer occurs preferentially through methyl branching of a monomethyl-branched isomer having already the more centrally positioned methyl group rather than the one close to the extremity of the chain. These peculiar positional selectivities and reaction paths can be explained by key-lock catalysis in pairs of micropore openings on the external surface of the ZSM-22 zeolite crystals.

Key Words: **ZSM-22; long *n*-alkanes; hydroisomerization; key-lock catalysis.**

INTRODUCTION

The development of efficient catalysts for skeletal branching of long *n*-alkanes without cracking is a scientific challenge. Catalysts on which the highest yields of skeletal isomers from model long *n*-alkanes were obtained are molybdenum oxycarbides (1, 2) and noble metal loaded acid zeolites having uniform tubular pores with diameters of about 0.5 nm (1, 3–14). The zeolite catalysts favor the formation of methyl branchings in the linear aliphatic hydrocarbon chains. On the Pt/H–ZSM-22 zeolite, the first methyl branching is formed preferentially at C_2–C_3 positions for decane and shorter *n*-alkanes and at C_2–C_3 or C_5–C_{11} positions of longer alkanes (9). Computational simulation of adsorption and self-diffusion of isoalkanes inside the pores of the zeolite crystals (15–19) led to the suggestion that diffusion-limited intracrystalline catalysis and transition state shape-selective effects were at the origin of the observed methyl-branching selectivity patterns. Experimentally determined and estimated physisorption equilibria of methylalkanes (9, 20, 21) and kinetic models of the catalytic conversions (22) were in favor of catalytic turnovers effected by acid sites in pore mouths. According to the latter explanation, the linear carbon chain penetrates with one end into a pore opening (pore mouth) or with both ends each into a different pore opening (key lock). The skeletal branching occurs on an acid site located in the pore very near the pore entrance. The pore mouth mode favors skeletal branching at C_2 and C_3 positions and the key-lock mode at C_5–C_{11}. The combination of pore mouth and key-lock mechanisms explains the observed bimodal reaction product distributions of monomethyl-branched skeletal isomers formed out of long *n*-alkanes from decane to tetracosane (9). In the favored dimethyl-branched isomers obtained by skeletal isomerization of C_{10}–C_{17} *n*-alkanes on Pt/H–ZSM-22, the two methyl groups are attached at carbon positions of the main chain that are far from each other (8,23), which was interpreted as another manifestation of key-lock catalysis.

In the present work we spent the effort to analyze in detail the multibranched isoalkanes obtained by isomerization of *n*-alkanes in the range from decane to tetracosane over Pt/ZSM-22 catalyst. This tedious task led to the discovery of peculiar skeletal branching patterns.

EXPERIMENTAL

The preparation and activation of Pt/ZSM-22 zeolite sample with a Si/Al ratio of 30 in the hydrogen form and the loading with 0.3 wt% of platinum metal with 14% dispersion were described earlier in this journal (9).

The reaction products originated from catalytic experiments published in (9). The feedstock consisted of an *n*-alkane in the range from decane to octadecane, eicosane,

0021-9517/01 $35.00

docosane, or tetracosane with more than 99% purity and heptane as diluent. The partial pressure of hydrogen (P_{H2}) was 418 kPa and that of hydrocarbon (P_{HC}) 32 kPa, giving an overall $P_{H2} : P_{HC}$ ratio of 13.1. The reaction temperature was 233°C. The space time, W/F_o, was varied by altering either the catalyst weight, W (g), or the molar flow rate F_o (mol s^{-1}) of the long *n*-alkane at the entrance of the catalyst bed. Reaction products were analyzed online with GC. Condensed reaction product samples were analyzed using a GC/MS instrument (Interscience quadrupole MD800 with electron impact). The capillary columns for the GC analysis had an internal diameter of 0.32 mm, length of 60 m, film thickness of 1.31 μm, and CP-Sil-5CB stationary phase (Chrompack). Monomethyl-branched isoalkanes eluted from the column in a specific sequence. The more the methyl group is positioned toward the end of the chain, the longer the retention time, with the exception that a 2-methyl-branched isomer elutes after a 3-methyl-branched isomer. The majority of the higher branched skeletal feed isomers were dimethyl-branched. A minor amount of methyl-/ethyl-branched isomers was detected, but the methyl and ethyl positions in these isomers could not be unambiguously determined. In the chromatograms, many peaks of dibranched isomers were overlapping. Detection of the presence of different compounds in the same peak was done by taking MS spectra at different positions in the peak. After careful identification of the skeletal isomerization products obtained with different *n*-alkanes, we discovered that the elution sequences of monomethyl-branched isomers also apply to dimethyl-branched isomers, provided the two methyl substituents are sufficiently separated from each other along the main chain. Chromatograms of the skeletal isomerization products obtained at high conversions of the respective *n*-alkanes and the peak assignment are given in the Appendix. The fraction of unidentified skeletal isomers increased with the chain length but remained relatively small; for example, in the experiment with *n*-C_{22}, it was ca. 25% at 99.5% conversion.

RESULTS AND DISCUSSION

The contact time of the long *n*-alkane was varied at a reaction temperature of 233°C. Monobranching, multibranching, and cracking were observed as consecutive reactions. The yield curves of monobranched and multibranched skeletal isomers and of the total of isomers from the long *n*-alkane fed to the reactor exhibited each a maximum value at a specific conversion level. These maximum yields and the contact times at which they were reached are listed in Table 1. The maximum yield of total isomers was 77–90%, confirming the excellent *n*-alkane skeletal isomerization properties of Pt/H–ZSM-22 catalyst. The maximum yield of monobranched isomers obtained with the different *n*-alkanes was 55–80% and not changing systematically with the carbon number. The maximum yield of multibranched isomers increased with the carbon number from 22% with *n*-C_{10} to over 70% with *n*-C_{20}, *n*-C_{22}, and *n*-C_{24}.

Typical distributions of the monobranched and identified dimethyl-branched isomerization products obtained under reaction conditions resulting in high yields of multibranched isomers are reported in Tables 2.1–2.12. The distribution of monobranched isomerization products was discussed in detail in (9) and reflects the selectivity

TABLE 1

Maximum Yield of Total Isomers (Y_{iso}), Monobranched Isomers (Y_{mono}), and Multibranched Isomers (Y_{multi}) in the Isomerization of Long *n*-Alkanes on Pt/H–ZSM-22

n-C_{n-2}	W/F_0 (kg s mol^{-1})	Y_{iso} (%)	W/F_0 (kg s mol^{-1})	Y_{mono} (%)	W/F_0 (kg s mol^{-1})	Y_{multi} (%)
n-C_{10}	690	78.5	690	68.9	3020	22.4
n-C_{11}	710	79.5	680	66.6	2140	31.6
n-C_{12}	1140	81.1	620	67.1	1980	30.0
n-C_{14}	890	83.2	690	62.9	1310	49.2
n-C_{15}	1320	83.6	590	68.5	1320	42.0
n-C_{16}	1870	78.9	1170	64.1	2660	35.3
n-C_{17}	2050	79.0	1320	63.5	2570	46.7
n-C_{18}	2190	88.0	1800	72.7	5170	48.4
n-C_{20}	3560	90.4	1970	80.5	5310	71.4
n-C_{22}	2300	88.7	1890	76.3	3750	77.3
n-C_{24}	2560	81.5	1920	54.9	3200	78.9

TABLE 2.1

Distribution of Monobranched and Dibranched C_{10} Isomers; X = 94.9%, Y_{iso} = 64.9%, Y_{crack} = 30.1%, Y_{mono} = 42.5%, and Y_{multi} = 22.4%

Compound	Position of branching	Distribution of monobranched isomers (wt%)
5-Methylnonane	5	12.4
4-Methylnonane	4	24.9
3-Methylnonane	3	29.0
2-Methylnonane	2	26.7
4-Ethyloctane	4	4.0
3-Ethyloctane	3	2.9
Compound	**Position of branchings[a]**	**Distribution of dibranched isomers (wt%)**
2,7-Dimethyloctane	2–2	24.8
2,6-Dimethyloctane	2–3	30.6
2,5-Dimethyloctane	2–4	16.9
2,4-Dimethyloctane	2–5	11.0
2,3-Dimethyloctane	2–6	3.8
2,2-Dimethyloctane	2–7	0.8
3,6-Dimethyloctane	3–3	7.8
3,5-Dimethyloctane	3–4	2.3
3,4-Dimethyloctane	3–5	1.9

[a] Counting from the two ends of the main chain.

TABLE 2.2

Distribution of Monobranched and Dibranched C_{11} Isomers; X = 95.1%, Y_{iso} = 71.7%, Y_{crack} = 23.4%, Y_{mono} = 43.5%, and Y_{multi} = 28.2%

Compound	Position of branching	Distribution of monobranched isomers (wt%)
5-Methyldecane	5	23.4
4-Methyldecane	4	22.8
3-Methyldecane	3	26.8
2-Methyldecane	2	24.4
3-Ethylnonane	3	2.6
Compound	**Position of branchings[a]**	**Distribution of dibranched isomers (wt%)**
2,8- + 3,6-Dimethylnonane	2–2 + 3–4	26.4
2,7-Dimethylnonane	2–3	28.9
2,6-Dimethylnonane	2–4	13.0
2,5-Dimethylnonane	2–5	12.6
2,4-Dimethylnonane	2–6	9.2
3,7-Dimethylnonane	3–3	7.9
3,5-Dimethylnonane	3–5	2.0

[a] Counting from the two ends of the main chain.

patterns mentioned in the introduction. Distributions of dimethyl-branched skeletal isomers given in Tables 2.1–2.12 at specific conversion levels did not change much with conversion, as illustrated for *n*-C_{18} in Fig. 1.

With all chain lengths studied, the 2,*n*dMe–C_{x-2} and 3,*n*dMe–C_{x-2} isomers were most abundantly formed. In

TABLE 2.3

Distribution of Monobranched and Dibranched C_{12} Isomers; X = 94.6%, Y_{iso} = 78.8%, Y_{crack} = 15.8%, Y_{mono} = 53.2%, and Y_{multi} = 25.7%

Compound	Position of branching	Distribution of monobranched isomers (wt%)
6- + 5-Methylundecane	6 + 5	31.6
4-Methylundecane	4	20.1
3-Methylundecane	3	24.3
2-Methylundecane	2	24.0
Compound	**Position of branchings[a]**	**Distribution of dibranched isomers (wt%)**
2,9-Dimethyldecane	2–2	24.4
2,8-Dimethyldecane	2–3	23.7
2,7-Dimethyldecane	2–4	15.9
2,6-Dimethyldecane	2–5	23.2
2,5-Dimethyldecane	2–6	6.3
2,4-Dimethyldecane	2–7	0.9
3,8-Dimethyldecane	3–3	4.7
3,7-Dimethyldecane	3–4	0.2
3,3-Dimethyldecane	3–8	0.7

[a] Counting from the two ends of the main chain.

TABLE 2.4

Distribution of Monobranched and Dibranched C_{13} Isomers; X = 95.2%, Y_{iso} = 76.0%, Y_{crack} = 19.1%, Y_{mono} = 54.7%, and Y_{multi} = 21.3%

Compound	Position of branching	Distribution of monobranched isomers (wt%)
6-Methyldodecane	6	18.4
5-Methyldodecane	5	20.0
4-Methyldodecane	4	18.2
3-Methyldodecane	3	22.3
2-Methyldodecane	2	21.1
Compound	**Position of branchings[a]**	**Distribution of dibranched isomers (wt%)**
2,10-Dimethylundecane	2–2	23.9
2,9-Dimethylundecane	2–3	16.2
2,8- + 4,8-Dimethylundecane	2–4 + 4–4	16.5
2,7-Dimethylundecane	2–5	12.1
2,6-Dimethylundecane	2–6	18.5
2,5-Dimethylundecane	2–7	6.5
2,4-Dimethylundecane	2–8	1.3
3,9-Dimethylundecane	3–3	3.4
3,6-Dimethylundecane	3–6	1.5

[a] Counting from the two ends of the main chain.

TABLE 2.5

Distribution of Monobranched and Dibranched C_{14} Isomers; X = 95.9%, Y_{iso} = 83.2%, Y_{crack} = 12.7%, Y_{mono} = 51.6%, and Y_{multi} = 31.6%

Compound	Position of branching	Distribution of monobranched isomers (wt%)
7- + 6-Methyltridecane	7 + 6	31.9
5-Methyltridecane	5	20.3
4-Methyltridecane	4	19.2
3-Methyltridecane	3	24.2
2-Methyltridecane	2	24.7
Compound	**Position of branchings[a]**	**Distribution of dibranched isomers (wt%)**
2,11-Dimethyldodecane	2–2	16.8
2,10-Dimethyldodecane	2–3	13.6
2,9- + 4,9-Dimethyldodecane	2–4 + 4–4	11.2
2,8- + 5,8-Dimethyldodecane	2–5 + 5–5	13.4
2,7-Dimethyldodecane	2–6	9.2
2,6-Dimethyldodecane	2–7	12.2
2,5-Dimethyldodecane	2–8	6.5
2,4-Dimethyldodecane	2–9	1.1
3,10-Dimethyldodecane	3–3	4.0
3,7-Dimethyldodecane	3–6	5.4
4,8-Dimethyldodecane	4–5	2.1
4,7-Dimethyldodecane	4–6	1.9
4,6-Dimethyldodecane	4–7	1.6
5,7-Dimethyldodecane	5–6	1.0

[a] Counting from the two ends of the main chain.

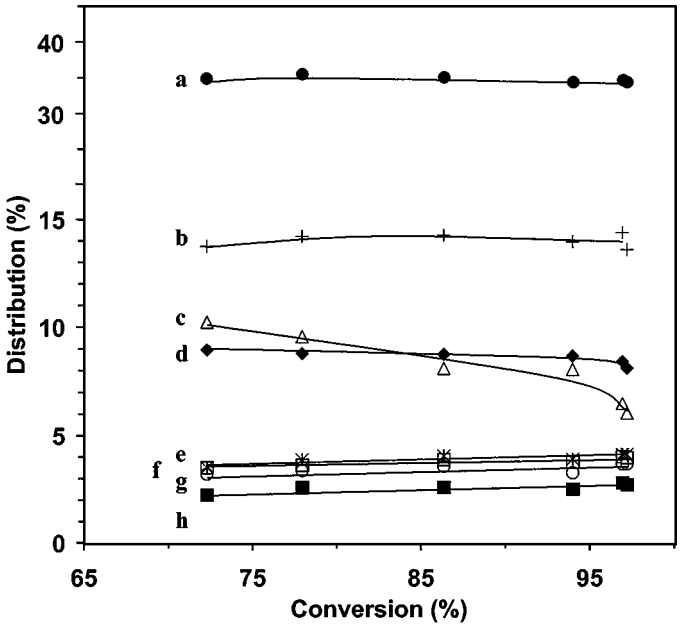

FIG. 1. Distribution of dimethylhexadecanes obtained at increasing conversion levels of octadecane on Pt/H–ZSM-22 catalyst: (a) 2,10dMe–C_{16} + 2,9dMe–C_{16} + 2,8dMe–C_{16}; (b) 2,11dMe–C_{16} + 6,11dMe–C_{16}; (c) 4,13dMe–C_{16} + 2,13dMe–C_{16} + 3,12dMe–C_{16} + 3,11dMe–C_{16}; (d) 3,14dMe–C_{16}; (e) 2,12dMe–C_{16} + 5,12dMe–C_{16}; (f) 3,13dMe–C_{16}; (g) 3,10dMe–C_{16}; (h) 3,9dMe–C_{16}.

TABLE 2.6

Distribution of Monobranched and Dibranched C_{15} Isomers; X = 94.7%, Y_{iso} = 83.6%, Y_{crack} = 11.1%, Y_{mono} = 63.8%, and Y_{multi} = 19.8%

Compound	Position of branching	Distribution of monobranched isomers (wt%)
7- + 6-Methyltetradecane	7 + 6	33.3
5-Methyltetradecane	5	15.8
4-Methyltetradecane	4	15.1
3-Methyltetradecane	3	18.4
2-Methyltetradecane	2	17.4
4-Ethyltridecane	4	Traces
Compound	Position of branchings[a]	Distribution of dibranched isomers (wt%)
2,12-Dimethyltridecane	2–2	14.5
2,11- + 3,10-Dimethyltridecane	2–3 + 3–4	16.6
2,10- + 4,10-Dimethyltridecane	2–4 + 4–4	11.6
2,9- + 5,9-Dimethyltridecane	2–5 + 5–5	12.8
2,8- + 6,8-Dimethyltridecane	2–6 + 6–6	20.9
2,7- + 2,6-Dimethyltridecane	2–7 + 2–8	10.6
3,11-Dimethyltridecane	3–3	2.3
3,9-Dimethyltridecane	3–5	3.0
4,9-Dimethyltridecane	4–5	2.6
4,8-Dimethyltridecane	4–6	1.8
4,7-Dimethyltridecane	4–7	1.0
5,8-Dimethyltridecane	5–6	1.0
6,7-Dimethyltridecane	6–7	1.3

[a] Counting from the two ends of the main chain.

TABLE 2.7

Distribution of Monobranched and Dibranched C_{16} Isomers; X = 95.2%, Y_{iso} = 79.2%, Y_{crack} = 16.0%, Y_{mono} = 56.8%, and Y_{multi} = 22.4%

Compound	Position of branching	Distribution of monobranched isomers (wt%)
8- + 7-Methylpentadecane	8 + 7	24.4
6-Methylpentadecane	6	12.7
5-Methylpentadecane	5	14.4
4-Methylpentadecane	4	13.2
3-Methylpentadecane	3	17.2
2-Methylpentadecane	2	18.1
4-Ethyltetradecane	4	Traces
Compound	Position of branchings[a]	Distribution of dibranched isomers (wt%)
2,13- + 3,11-Dimethyltetradecane	2–2 + 3–4	14.1
2,12- + 3,12-Dimethyltetradecane	2–3 + 3–3	13.0
2,11- + 4,11-Dimethyltetradecane	2–4 + 4–4	10.1
2,10- + 3,8- + 5,10-Dimethyltetradecane	2–5 + 3–7 + 5–5	11.7
2,9- + 2,8- + 2,7-Dimethyltetradecane	2–6 + 2–7 + 2–8	26.5
3,9-Dimethyltetradecane	3–6	3.7
3,7- + 6,9-Dimethyltetradecane	3–8 + 6–6	9.5
4,10-Dimethyltetradecane	4–5	1.8
4,9- + 4,8- + 4,7-Dimethyltetradecane	4–6 + 4–7 + 4–8	2.6
5,9- + 5,8-Dimethyltetradecane	5–6 + 5–7	3.7
6,8-Dimethyltetradecane	6–7	2.3
6,7-Dimethyltetradecane	6–8	1.0

[a] Counting from the two ends of the main chain.

n-C_{10}, n-C_{11}, and n-C_{12} conversions, no other dimethyl-branched isomers were formed but 2,ndMe–C_{x-2}. Formation of 4,ndMe–C_{x-2} and 5,ndMe–C_{x-2} isomers was observed with n-alkanes with minimum lengths of 13 and 14 carbon atoms, respectively. The 4,ndMe–C_{x-2} isomer fraction was always more abundant than the 5,ndMe–C_{x-2} fraction. Isomers of the type 6,ndMe–C_{x-2} appear with n-C_{15} alkanes and longer and 7,ndMe–C_{x-2} isomers with n-C_{18} and longer. The 6,ndMe–C_{x-2} and 7,ndMe–C_{x-2} isomers were formed in minor amounts.

The following criterion was handled to distinguish between the most favored and less favored dimethyl-branched isomers. The most abundant isomer and all other isomers representing more than 50% of the weight of the most abundant isomer in the reaction product mixtures were considered as "most favored". Isomers representing between 25 and 50% of the weight of the most abundant isomer were counted among the "less favored" isomers. The preferred positions for the methyl branchings in the dimethyl-branched skeletal isomers are schematically represented in Fig. 2A–2L. The number of most preferred isomers is generally limited but tends to increase with the carbon

TABLE 2.8

Distribution of Monobranched and Dibranched C_{17} Isomers; X = 94.8%, Y_{iso} = 70.5%, Y_{crack} = 24.3%, Y_{mono} = 52.0%, and Y_{multi} = 18.5%

Compound	Position of branching	Distribution of monobranched isomers (wt%)
8- + 7- + 6-Methylhexadecane	8 + 7 + 6	44.7
5-Methylhexadecane	5	11.5
4-Methylhexadecane	4	12.0
3-Methylhexadecane	3	15.8
2-Methylhexadecane	2	16.6
4-Ethylpentadecane	4	Traces
Compound	**Position of branchings[a]**	**Distribution of dibranched isomers (wt%)**
2,14- + 3,12-Dimethylpentadecane	2–2 + 3–4	15.9
2,13- + 3,13-Dimethylpentadecane	2–3 + 3–3	10.5
2,12- + 4.12-Dimethylpentadecane	2–4 + 4–4	6.6
2,11- + 3,10- + 5,11-Dimethylpentadecane	2–5 + 3–6 + 5–5	11.8
2,10- + 2,9- + 2,8- + 2,7- + 6,10-Dimethylpentadecane	2–6 + 2–7 + 2–8 + 2–9 + 6–6	36.3
4,10-Dimethylpentadecane	4–6	2.5
4,9- + 4,8-Dimethylpentadecane	4–7 + 4–8	6.0
4,7-Dimethylpentadecane	4–9	4.0
5,10-Dimethylpentadecane	5–6	0.6
5,9- + 5,8-Dimethylpentadecane	5–7 + 5–8	1.8
6,9- + 6,8-Dimethylpentadecane	6–7 + 6–8	2.1
7,9-Dimethylpentadecane	7–7	1.9

[a] Counting from the two ends of the main chain.

number. There are 2 most preferred isomers formed out of *n*–C_{10} and 20 from *n*-C_{24}. In the conversion of *n*-C_{10}–*n*-C_{16} feedstocks, the most preferred isomers were found in the 2,*n*dMe–C_{x-2} family (Figs. 2A–2G). For *n*-C_{17} (Fig. 2H) and *n*-C_{18} (Fig. 2I), the most preferred isomers occur in he 2,*n*dMe–C_{x-2} and 3,*n*dMe–C_{x-2} isomer families. For *n*-C_{20} (Fig. 2J) and *n*-C_{22} (Fig. 2K) the 4,*n*dMe–C_{x-2} fraction also contains most abundant isomers. For *n*-C_{24} (Fig. 2L) even the 6,*n*dMe–C_{x-2} fraction contains a most abundant isomer.

In the most preferred skeletal isomers, the tertiary carbon atoms carrying the methyl groups were separated by at least three methylene groups (2,6dMe–C_{x-2} isomer with x equal to 10, 12, 13, and 14 (Figs. 2A and 2C–2E)), and at the maximum 14 methylene carbon atoms (3,18dMe–C_{20} isomer (Fig. 2K)). The minimum spacing between the tertiary carbon atoms was dependent on the chain length. For the 2,*n*dMe–C_{x-2} fraction, it varies from three carbon atoms for the shortest chains to five carbon atoms for the longest chains (Figs. 2A–2L). In the most favored isomers of the 3,*n*dMe–C_{x-2} and 4,*n*dMe–C_{x-2} families, the minimum spacing of the branchings corresponds also to four and five carbon atoms (Figs. 2J–2L).

In the 2,*n*dMe–C_{x-2} family, the preferred position for the second branching is located at carbon atoms in the range C_6–C_{14} (Figs. 2A–2L). More separated positions for the methyl groups are not favored.

The 3,*n*dMe–C_{x-2} family shows different behavior. In the experiments with *n*–C_{20}, *n*-C_{22}, and *n*-C_{24} (Figs. 2J–2L), there were clearly two ranges of positions along the chain for the positioning of the second methyl group. The first range of preferred positions is C_8–C_{12} and the second range is at C_{16}–C_{20}.

The 4,*n*dMe–C_{x-2} family was abundantly formed in the conversion of *n*-C_{24} (Fig. 2L). Unfortunately, the 4,*n*dMe–C_{22} isomers with *n* equal to 8–16 eluted together from the GC column. In Fig. 2L, all these positions were indicated as most favored based on the total weight of these compounds in the product, but it is likely that these isomers were not all

TABLE 2.9

Distribution of Monobranched and Dibranched C_{18} Isomers; X = 96.8%, Y_{iso} = 87.1%, Y_{crack} = 9.7%, Y_{mono} = 54.2%, and Y_{multi} = 32.9%

Compound	Position of branching	Distribution of monobranched isomers (wt%)
9- + 8-Methylheptadecane	9 + 8	23.5
7-Methylheptadecane	7	12.8
6-Methylheptadecane	6	13.1
5-Methylheptadecane	5	12.5
4-Methylheptadecane	4	11.2
3-Methylheptadecane	3	13.4
2-Methylheptadecane	2	13.5
4-Ethylhexadecane	4	Traces
Compound	**Position of branchings[a]**	**Distribution of dibranched isomers (wt%)**
2,13- + 3,12- + 3,11- + 4,13-Dimethylhexadecane	2–4 + 3–5 + 3–6 + 4–4	6.6
2,12- + 5,12-Dimethylhexadecane	2–5 + 5–5	4.2
2,11- + 6,11-Dimethylhexadecane	2–6 + 6–6	14.5
2,10- + 2,9- + 2,8-Dimethylhexadecane	2–7 + 2–8 + 2–9	34.7
3,14-Dimethylhexadecane	3–3	8.5
3,13-Dimethylhexadecane	3–4	4.1
3,10-Dimethylhexadecane	3–7	3.8
3,9-Dimethylhexadecane	3–8	2.8
4,11-Dimethylhexadecane	4–6	
4,10- + 4,9-Dimethylhexadecane	4–7 + 4–8	3.3
4,8-Dimethylhexadecane	4–9	4.4
5,11-Dimethylhexadecane	5–6	2.2
5,10- + 5,9- + 5,8-Dimethylhexadecane	5–7 + 5–8 + 5–9	4.7
6,10- + 6,9-Dimethylhexadecane	6–7 + 6–8	4.2
7,10-Dimethylhexadecane	7–7	2.0

[a] Counting from the two ends of the main chain.

TABLE 2.10

Distribution of Monobranched and Dibranched C_{20} Isomers; X = 96.4%, Y_{iso} = 90.4%, Y_{crack} = 6.0%, Y_{mono} = 46.2%, and Y_{multi} = 44.2%

Compound	Position of branching	Distribution of monobranched isomers (wt%)
10- + 9- + 8-Methylnonadecane	10 + 9 + 8	31.8
7-Methylnonadecane	7	12.5
6-Methylnonadecane	6	11.6
5-Methylnonadecane	5	10.7
4-Methylnonadecane	4	9.5
3-Methylnonadecane	3	12.0
2-Methylnonadecane	2	12.0
Compound	**Position of branchings[a]**	**Distribution of dibranched isomers (wt%)**
2,16- + 3,15-Dimethyloctadecane	2–3 + 3–4	3.1
2,15- + 3,14-Dimethyloctadecane	2–4 + 3–5	9.3
2,14- + 3, 12- + 5,14-Dimethyloctadecane	2–5 + 3–7 + 5–5	8.2
2,13- + 3,10- + 3,9- + 6,13-Dimethyloctadecane	2–6 + 3–9 + 3–10 + 6–6	25.4
2,12- + 2,11- + 2,10- + 2,9- + 2,8-Dimethyloctadecane	2–7 + 2–8 + 2–9 + 2–10 + 2–11	24.5
3,16-Dimethyloctadecane	3–3	9.2
3,13-Dimethyloctadecane	3–6	3.2
4,15-Dimethyloctadecane	4–4	6.3
4,13-Dimethyloctadecane	4–6	0.7
4,12-Dimethyloctadecane	4–7	2.8
4,11-Dimethyloctadecane	4–8	1.3
4,10- + 4,9- + 4,8-Dimethyloctadecane	4–9 + 4–10 + 4–11	2.6
5,*n*-Dimethyloctadecane (n = 8 to 13)	5–*y* (y = 6 to 11)	2.7
6,*n*-Dimethyloctadecane (n = 9 to 12)	6–*y* (y = 7 to 10)	0.7

[a] Counting from the two ends of the main chain.

formed in the same quantity and that the number of most preferred isomers is smaller.

The preferred isomers contain many "symmetric" molecules, i.e., molecules with the two methyl groups at an equivalent position such as 2,*x*-3dMe–C_{x-2}, 3,*x*-4dMe–C_{x-2}, 4,*x*-5dMe–C_{x-2}, 5,*x*-6dMe–C_{x-2}, and 6,*x*-7dMe–C_{x-2}. In the 2,*n*dMe–C_{x-2} fractions, the 2,*x*-3dMe–C_{x-2} isomer dominates when the molecule has 16 carbon atoms or less (Figs. 2A–2G). In the 3,*n*dMe–C_{x-2} fraction, the 3,*x*-4dMe–C_{x-2} molecule is the most abundant isomer except with the heaviest alkane studied, viz., *n*-C_{24} (Figs. 2A–2L). In the 4,*n*dMe–C_{x-2} products, the 4,*x*-5dMe–C_{x-2} isomer is generally less dominant (Figs. 2G–2L). Isomers of the type 5,*x*-6dMe–C_{x-2} and 6,*x*-7dMe–C_{x-2} are the most preferred isomers of their respective fractions (Figs. 2G–2L).

A salient question regarding the formation of the nonsymmetric dimethylalkanes is whether they are formed out of the monobranched isomer with the more terminal methyl group or from the monobranched isomer having already the more centrally positioned methyl branching. The experiment with *n*-C_{14} was selected to investigate this issue. The content of the 2,*n*dMe–C_{12} isomer in the dimethyldodecane product fraction was plotted against the content of the different possible precursors among the monomethyl-branched skeletal isomers (Fig. 3). The following relationships were found. The formation of 2,11dMe–C_{12} shows a positive relation with the content of 2Me–C_{13} in the monobranched isomers, as expected since 2Me–C_{13} is the only possible precursor. The formation of all the other 2,*n*dMe–C_{12} isomers with *n* equal to 4, 5,

TABLE 2.11

Distribution of Monobranched and Dibranched C_{22} Isomers; X = 95.9%, Y_{iso} = 35.6%, Y_{crack} = 60.3%, Y_{mono} = 23.2%, and Y_{multi} = 12.5%

Compound	Position of branching	Distribution of monobranched isomers (wt%)
11- + 10- + 9- + 8-Methyluneicosane	11 + 10 + 9 + 8	37.7
7-Methyluneicosane	7	12.4
6-Methyluneicosane	6	10.0
5-Methyluneicosane	5	8.5
4-Methyluneicosane	4	7.6
3-Methyluneicosane	3	10.7
2-Methyluneicosane	2	13.1
3-Ethyleicosane	3	Traces
Compound	**Position of branchings[a]**	**Distribution of dibranched isomers (wt%)**
2,12- + 2,11- + 2,10- + 2,9- + 2,8- + 6,15- Dimethyleicosane	2–9 + 2–10 + 2–11 + 2–12 + 2–13 + 6–6	13.3
3,18-Dimethyleicosane	3–3	9.4
3,17-Dimethyleicosane	3–4	4.8
3,16- + 4,15-Dimethyleicosane	3–5 + 4–6	9.4
3,15-Dimethyleicosane	3–6	4.1
3,14- + 3,13- + 5,16-Dimethyleicosane	3–7 + 3–8 + 5–5	10.6
3,12- + 3,11- + 3,10- + 3,9- + 3,8-Dimethyleicosane	3–9 + 3–10 + 3–11 + 3–12 + 3–13	26.5
4,17-Dimethyleicosane	4–4	5.8
4,*n*-Dimethyleicosane (n = 7 to 14)	4–*y* (y = 7 to 14)	7.7
5,*n*-Dimethyleicosane (n = 8 to 15)	5–*y* (y = 6 to 13)	4.8
6,*n*-(n = 9 to 14) + 7,*n*-(n = 10 to 13) Dimethyleicosane	6–*y* (y = 7 to 12) + 7–*y* (y = 8 to 11)	3.6

[a] Counting from the two ends of the main chain.

TABLE 2.12

Distribution of Monobranched and Dibranched C_{24} Isomers; $X = 99.6\%$

Compound	Position of branching	Distribution of monobranched isomers(wt%)
12- + 11- + 10- + 9- + 8-Methyltricosane	12 + 11 + 10 + 9 + 8	50.9
7-Methyltricosane	7	8.5
6-Methyltricosane	6	12.4
5-Methyltricosane	5	7.0
4-Methyltricosane	4	6.7
3-Methyltricosane	3	7.8
2-Methyltricosane	2	6.7
3-Ethyldocosane	3	Traces
Compound	**Position of branchings[a]**	**Distribution of dibranched isomers (wt%)**
2,19- + 3,18- + 4,17-Dimethyldocosane	2–4 + 3–5 + 4–6	1.9
2,12- + 2,11- + 2,10- + 2,9- + 2,8-Dimethyldocosane	2–11 + 2–12 + 2–13 + 2–14 + 2–15	19.4
3,20- + 3,19-Dimethyldocosane	3–3 + 3–4	2.9
3,17- + 3,14-Dimethyldocosane	3–6 + 3–9	1.1
3,12- + 3,11- + 3,10- + 3,9- + 3,8-Dimethyldocosane	3–11 + 3–12 + 3–13 + 3–14 + 3–15	23.0
4,19-Dimethyldocosane	4–4	1.5
6,17-Dimethyldocosane	6–6	4.6
4,*n*-dimethyldocosane ($n = 7$ to 16)	4–*y* ($y = 7$ to 16)	38.7
5,*n*-Dimethyleicosane ($n = 8$ to 17)	5–*y* ($y = 6$ to 15)	7.6
6,*n*-($n = 9$ to 16) + 7, *n*-($n = 10$ to 15) Dimethyldocosane	6–*y* ($y = 7$ to 14) + 7–*y*($y = 8$ to 13)	2.2

[a] Counting from the two ends of the main chain.

6, 7, or 10 increases with increasing concentration of the precursor with the more centrally positioned monomethyl-branched isomer and not with 2Me–C_{13} (Fig. 3). The formation of dibranched isomers occurs preferentially from the monobranched isomer having already the most centrally positioned methyl group.

Based on simulation of the formation of dimethyl-branched alkane isomers inside the micropores of ZSM-22 using the Configurational Bias Monte Carlo approach, it was predicted that the reaction product mixtures would contain very little 2,6-dimethylalkanes and 2,10-dimethylalkanes and large amounts of 2,7-, 2,8-, and 2,9-dimethylalkanes (18). The presently reported experimental product distributions obtained with a wide variety of paraffins (Table 2, Fig. 2) are in disagreement with that prediction. For instance, in the conversion of *n*-C_{13}, the 2,10dMe–C_{11} and 2,6dMe–C_{11} were the two most important isomers (Table 2.4 and Fig. 2D).

The formation of dimethyl-branched isomers can be explained by key-lock catalysis as follows. Experimentally determined heats of adsorption of methylalkanes suggest that molecules adsorb with their methyl branching in the first undulation encountered in the pore (20–22). Contrary to the computational simulations (15–19), experimental adsorption data suggest that the branched molecules do not penetrate any deeper into the pores. For a ZSM-22 sample with a homogeneous atomic Si/Al ratio of 30 (9), there is an aluminum atom and an acid site associated with it in every set of three 10-rings delineating such undulation. Thus, there is a catalytic site in the first undulation of every pore. The formation of the second methyl branching in a monomethyl-branched isomer can then be pictured as follows. Depending on the position of the methyl side chain on the main chain, the methylalkane with its methyl group in the first undulation of one pore can enter with its other end of the main chain into a second pore, provided the main chain is sufficiently long. In this key-lock type of adsorbed state, the molecule undergoes its second methyl branching in the first undulation of the second pore.

There are two locks on the surface of ZSM-22 which are relevant to dimethyl branching of the chain lengths investigated (Fig. 4). The length of the bridge between the pore mouths of *lock a* corresponds to a chain of three methylene carbon atoms at least (23). In the *lock b*, a chain of at least eight carbon atoms is necessary to span the distance between the two openings. The dimethyl branching of C_{14} chains will be discussed first as an example. Abundantly formed dimethyl-branched isomers from *n*-C_{14} skeletal isomerisation are 2,*n*dMe–C_{12} with *n* equal to 6–11, having a chain composed of 3–8 carbon atoms between the tertiary carbon atoms carrying the methyl groups. These isomers fit with *lock a* and the largest one also with *lock b*, confirming that these locks serve as templates for the branching. The 2,8dMe–C_{12} isomer can be obtained by skeletal branching of either 2Me–C_{13} or 5Me–C_{13}. The adsorption of methyltetradecanes in *lock a* is schematically represented in Fig. 5. The 2Me–C_{13} molecule is only weakly adsorbed in the pore opening at the right as the methyl group at the C_2 position hampers the penetration (Fig. 5A). The interaction improves the more the methyl group is positioned in the center of the chain. For example, the 5Me–C_{13} molecule is held with an *n*-butyl group in the pore at the right (Fig. 5B). It explains the experimental observation (Fig. 3) that for the formation of a dimethyl-branched isomer, the monomethyl-branched isomer having already the more centrally positioned methyl group is a better precursor compared to the monomethyl-branched isomer having the methyl group close to the extremity of the chain.

The formation of dimethyl-branched isomers from longer *n*-alkanes such as *n*-C_{17} can be explained in a similar way

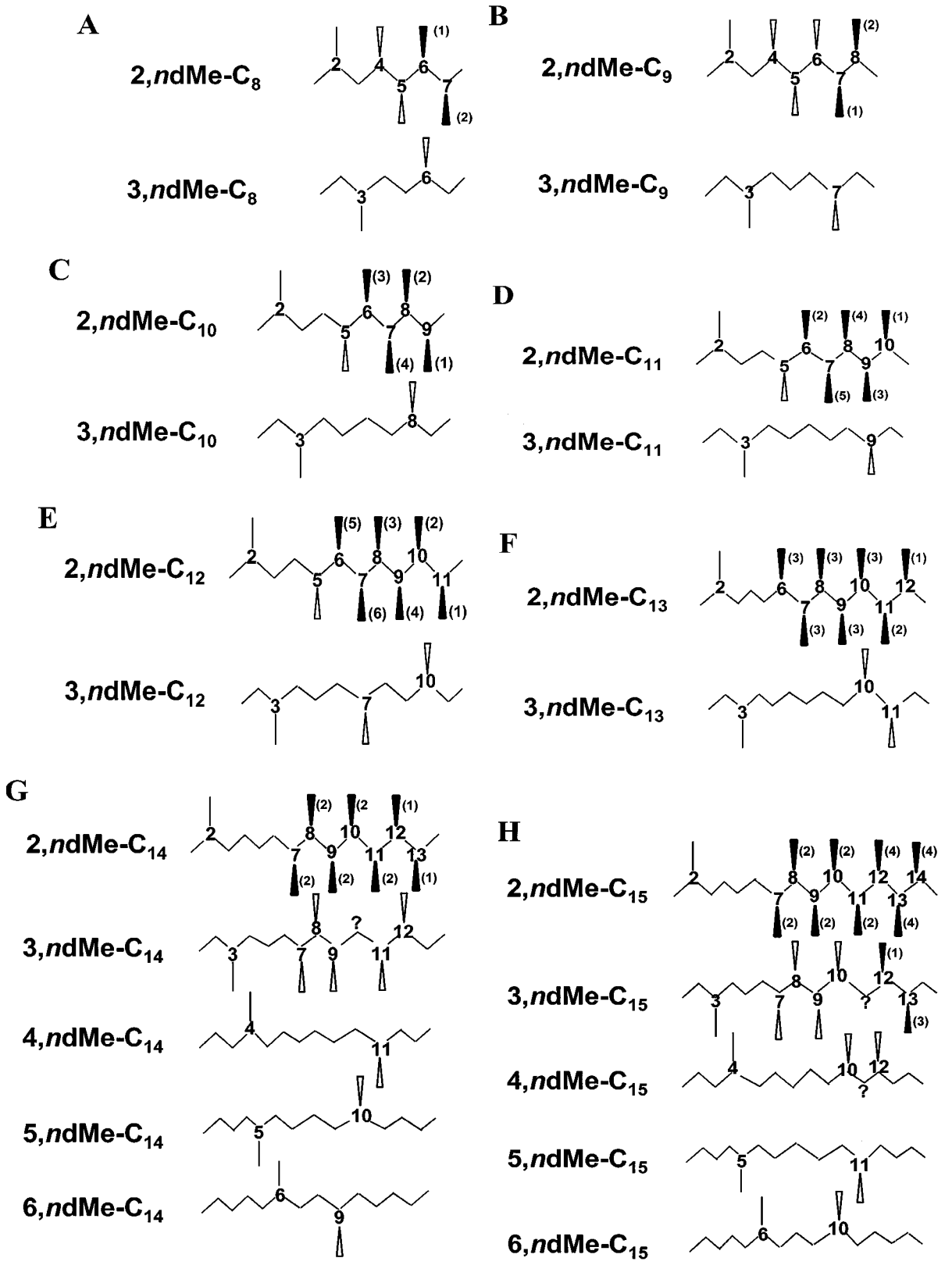

FIG. 2. Schematic representation of positional dimethyl-branching selectivity of *n*-C_{10}–*n*-C_{18} (A–I), *n*-C_{20} (J), *n*-C_{22} (K), and *n*-C_{24} (L) *n*-alkanes on Pt/H–ZSM-22 (data from Table 2.1–12). The position of the first methyl side chain is indicated with a bar. The solid arrows indicate the most favored positions for the second methyl group and the open arrows the less favored positions. Positions without arrows are unfavored. The numbers within brackets indicate the order of abundance of the most preferred isomers in the reaction products. Question marks indicate positions for which the GC peak was missing or strongly overlapped with others.

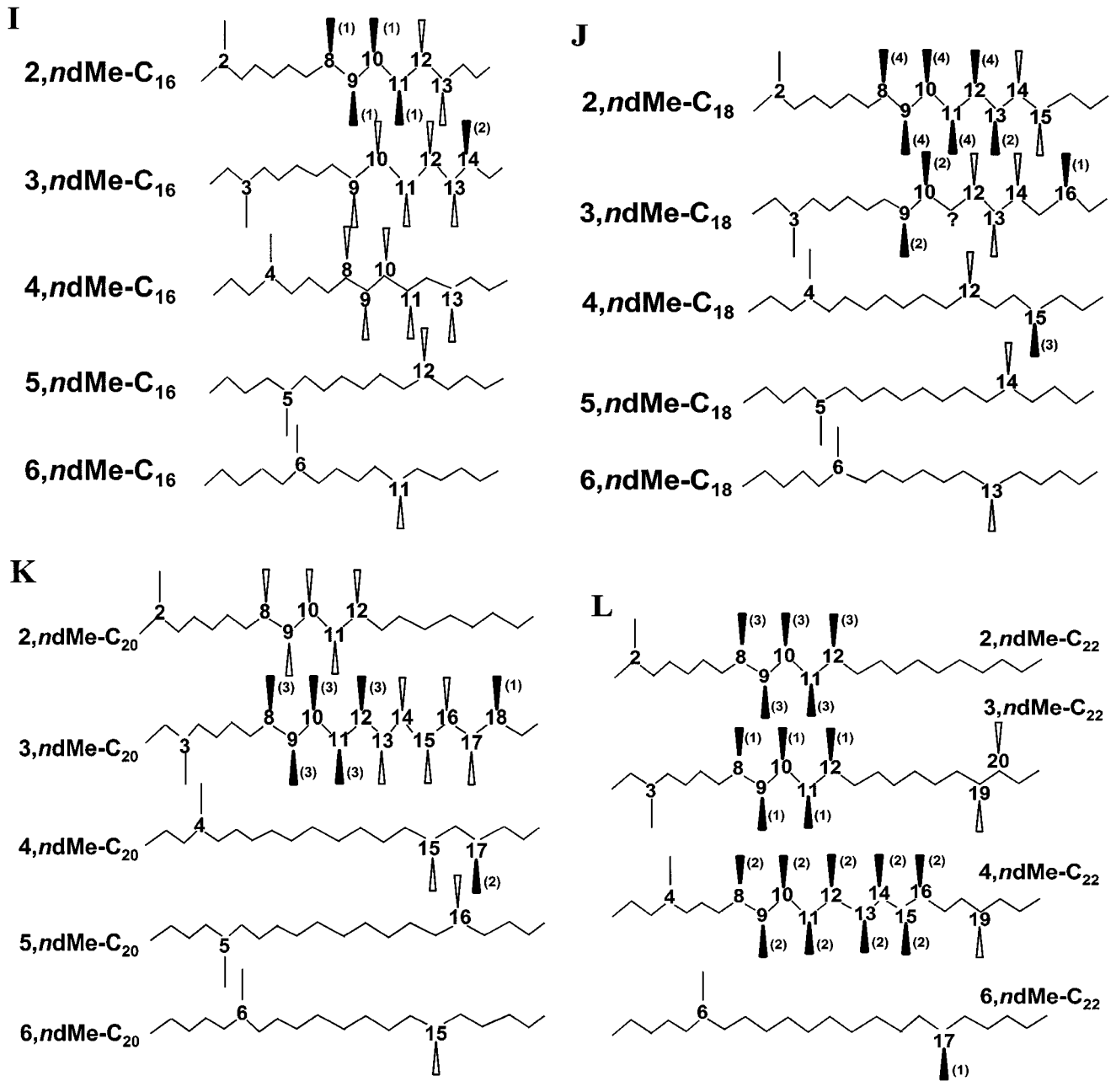

FIG. 2—*Continued*

based on key-lock conversions in locks *a* and *b*. The most abundant isomers are 2,*n*dMe–C_{15} with *n* from 7 to 14 and having a chain with 4 to 11 carbon atoms between the carbon atoms carrying the branchings and the 3,12dMe–C_{15} and 3,13dMe–C_{15} isomers with 8 and 9 carbon atoms between the branchings. Other less preferred isomers such as 3,*n*dMe–C_{15} with *n* from 7 to 11 and 4,*n*dMe–C_{15} with *n* from 10 to 12, 5,11dMe–C_{15} and 6,10dMe–C_{15} all have from 3 to 7 carbon atoms in the chain between the branching positions. The formation of the preferred isomers can be visualized as follows. For example, the 8Me–C_{16} molecule has *n*-alkyl groups with 7 and 8 carbon atoms. It can adsorb in two ways (Figs. 6A and 6B). The adsorption with the longest possible *n*-alkyl chain in the pore is preferred (9). In *lock a*, this adsorption mode gives rise to the formation of 2,7dMe–C_{15} and 3,7dMe–C_{15} (Fig. 6A). The alternative adsorption mode leads to the formation of 2,8dMe–C_{15}, 3,8dMe–C_{15}, and 4,8dMe–C_{15} when respecting the minimum of 3 carbon atoms in between the tertiary carbon atoms carrying the methyl groups (Fig. 6B).

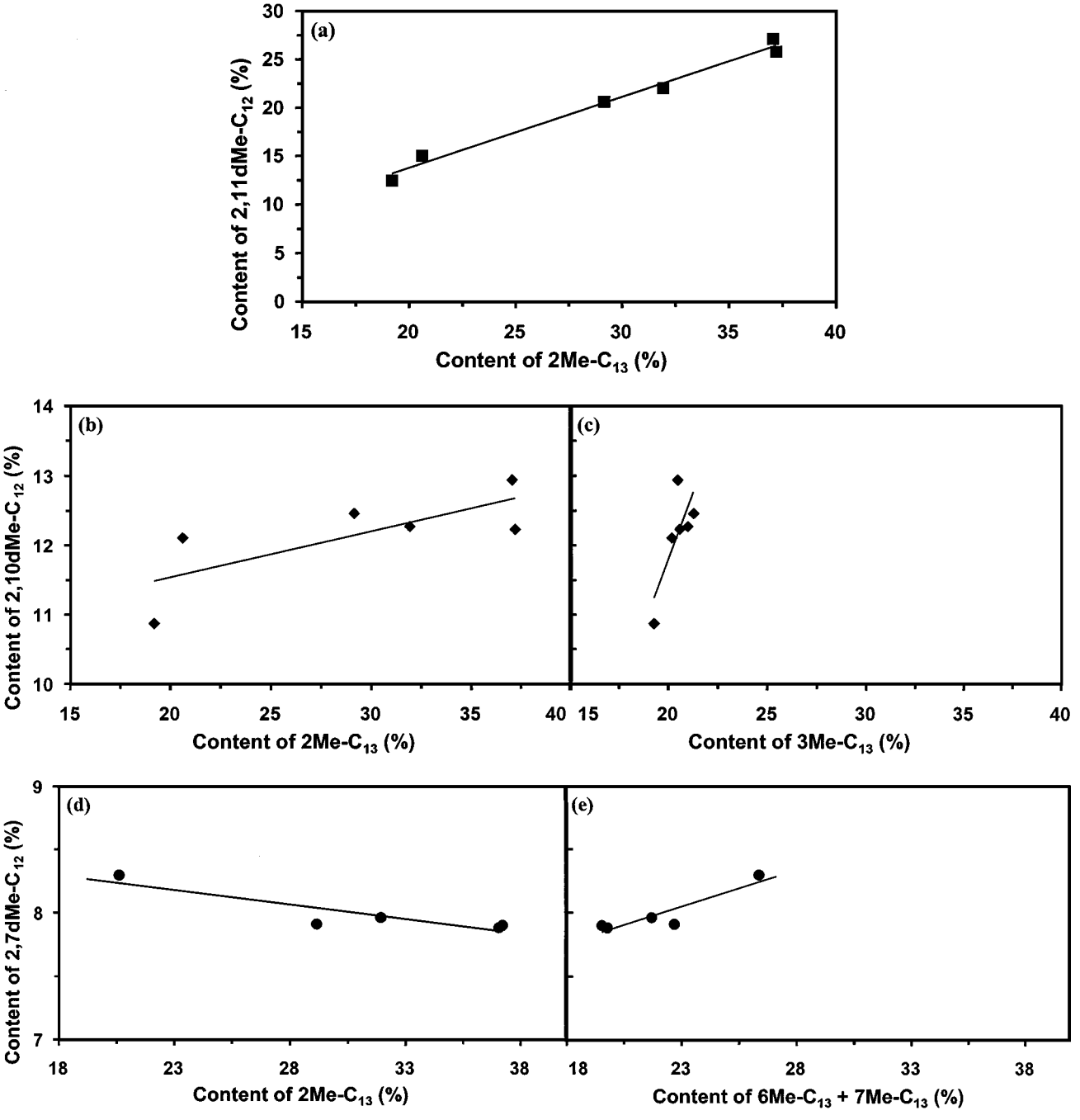

FIG. 3. Relationship between the content of the individual dimethyl-branched isomer in multibranched skeletal isomers and the content of the precursor monobranched isomer in monobranched skeletal isomers from *n*-C_{14} conversion.

The 2,12dMe–C_{15}, 2,13dMe–C_{15}, and 2,14dMe–C_{15} isomers are formed in *lock b* out of 4Me–C_{16}, 3Me–C_{16}, and 2Me–C_{16} monobranched isomers, respectively. In these isomers, there is a chain of 9, 10, and 11 carbon atoms between carbon atoms carrying the methyl groups. *Lock b* is also the locus for the formation of 3,12dMe–C_{15} and 3,13dMe–C_{15} isomers. The preferred reaction pathways for methyl branching of *n*-C_{17} in the locks of Pt/H–ZSM-22 catalyst are summarized in Fig. 7.

The preferential formation of symmetric isomers having the two methyl groups at equivalent carbon positions (2,*x*-3dMe–C_{x-2}, 3,*x*-4dMe–C_{x-2}, 4,*x*-5dMe–C_{x-2}, etc.) can be understood in terms of key-lock catalysis and an

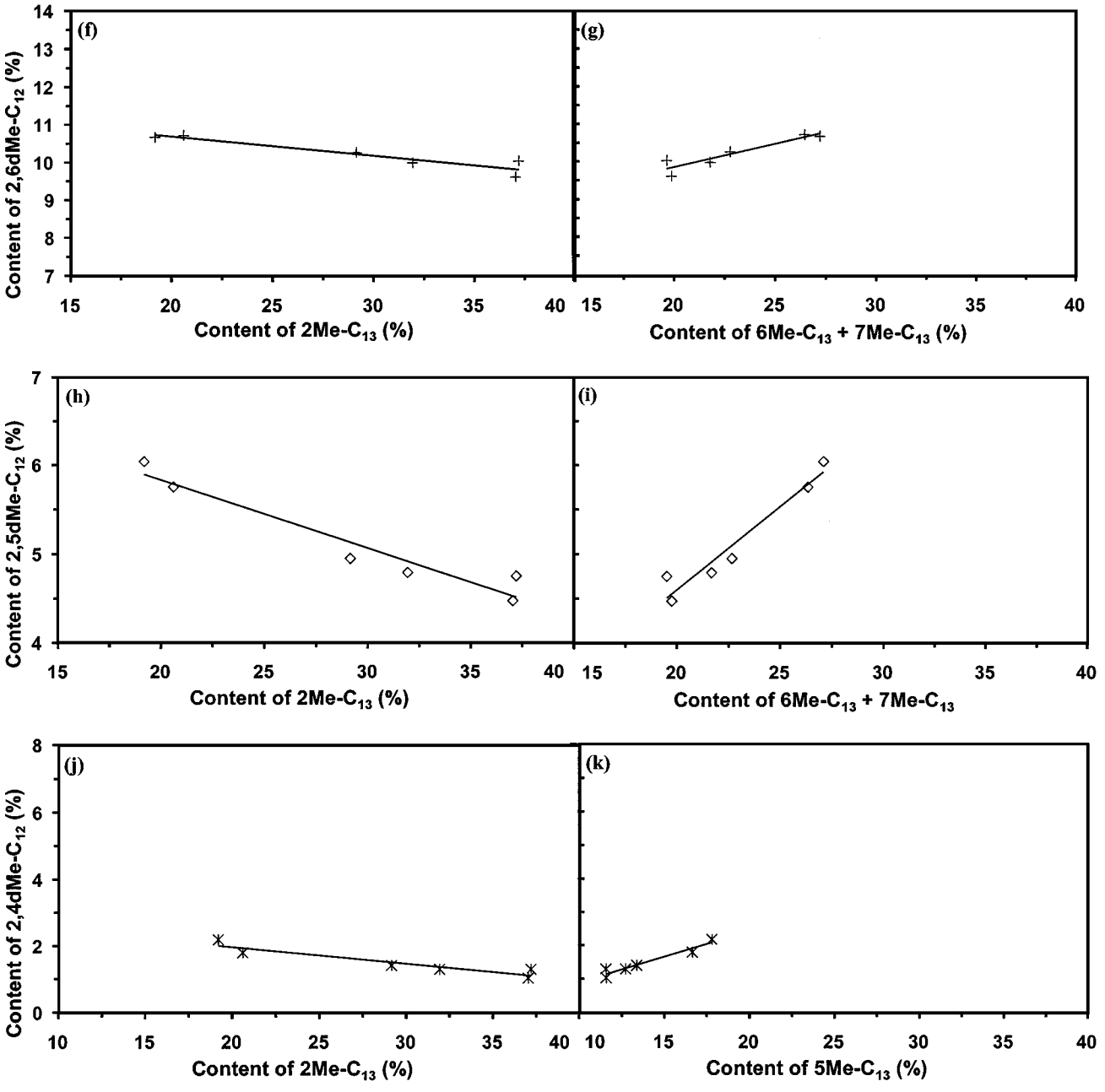

FIG. 3—*Continued*

equilibration of the interaction with the two parts of the lock.

Among the preferred 2,*n*dMe–C_{x-2} isomers obtained with the different *n*-alkanes, the largest value for *n* is 14 (obtained in the experiment with *n*-C_{17}, Fig. 2H), corresponding to a spacing by 12 carbon atoms along the chain. Preferred isomers with a larger distance between the branching positions in the chain were encountered in the 3,*n*dMe–C_{x-2} and 4,*n*dMe–C_{x-2} families obtained out of *n*-C_{20}, *n*-C_{22}, and *n*-C_{24} (Figs. 2J–2L). The key-lock model offers an explanation for this observation. For the formation of a branching at the C_2 position following the key-lock mode, only the last 4 carbons of the chain must penetrate into the pore. The farther the already existing methyl branching from this chain end, the larger the number of carbon atoms that cannot favorably interact with pore walls. The terminal methyl group of the 2Me–C_{x-1} molecules is also a weak anchor for holding the molecule

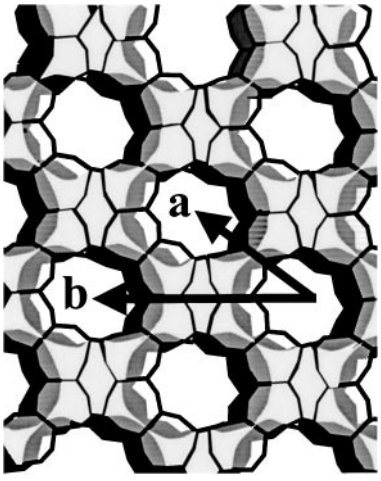

FIG. 4. Location of locks a and b on the surface of ZSM-22 crystals.

in one of the two pore mouths (cfr. Fig. 5A for 2Me–C_{13}). Ethyl, propyl, and bulkier groups of 3Me–C_{x-1}, 4Me–C_{x-1}, and more centrally branched isomers interact much more strongly in the pore mouth and are more suitable for fixing the branched part of the molecule in one of the two holes of the lock and to allow reaction in the other pore.

The nature of the preferred multibranched skeletal isomers from long *n*-alkanes offers an explanation of why the Pt/H–ZSM-22 catalyst has a low tendency for cracking (24). In the preferred isomers, the methyl groups are not in suitable positions to allow cracking via β-scission.

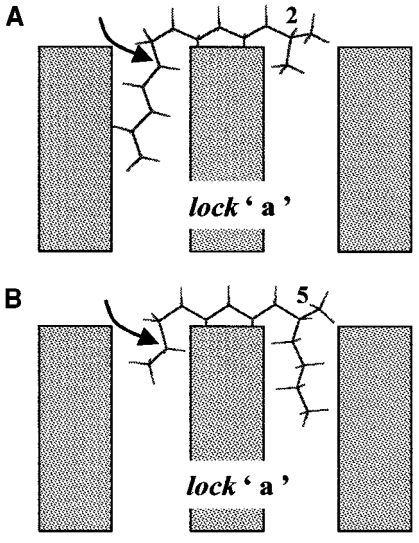

FIG. 5. Formation of 2,8dMe–C_{12} in lock a out of 2Me–C_{13} (A) and 5Me–C_{13} (B). The arrow indicates the position in the chain where branching will occur.

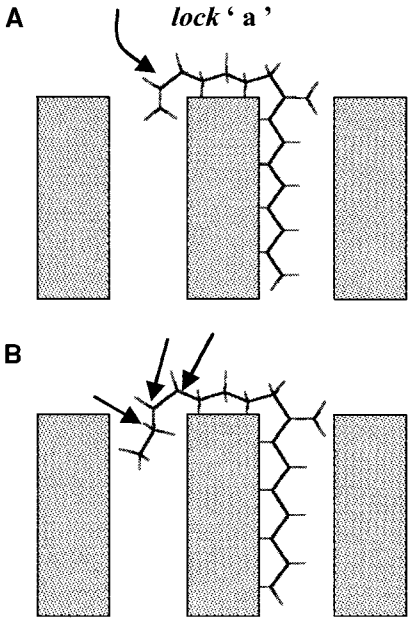

FIG. 6. Methyl branching of 8Me–C_{16} in lock a. Adsorption with eight carbons in a pore leads to the formation of 2,7dMe–C_{15} and 3,7dMe–C_{15} (A). Adsorption in (B) leads to the formation of 2,8dMe–C_{15}, 3,8dMe–C_{15}, and 4,8dMe–C_{15}.

CONCLUSIONS

Pt/H–ZSM-22 is an excellent catalyst for methyl branching and dimethyl branching of *n*-alkanes from decane to tetracosane. The positional selectivity of dimethyl branching is very peculiar. The second methyl branch is positioned on the monomethyl-branched isomer at carbon positions leaving preferably a chain of at least 3 and at most 14 carbon atoms between the branching positions. The formation of methyl branchings is a consecutive process. In molecules with nonequivalent methyl positions, first the most centrally positioned methyl group is formed and subsequently the methyl group near the end of the chain. The positional selectivity of dimethyl branching of *n*-alkanes can be rationalized with the key-lock catalysis concept. The monomethylalkane is adsorbed in a pore opening, with the tertiary carbon atom and the methyl side chain accommodated in the first slight enlargement encountered in the pore. The alkyl chain remaining outside this pore penetrates a neighboring pore mouth. The second methyl branch is generated on this part of the molecule at carbon positions located in the first lobe of that pore. Two neighboring pore mouths thus form a lock for the hydrocarbon molecule. With the range of chain lengths studied, two locks are operative. *Lock a* has the shortest distance between the two pore openings. Methylalkanes with 13 and less carbon atoms react in *lock a*. C_{14} and longer molecules react in *lock a* and *lock b*, having a much larger spacing between the pore openings.

With the shorter *n*-C_x alkanes, 2,*n*dMe–C_{x-2} isomers are preferentially formed. The longer the molecules, the more

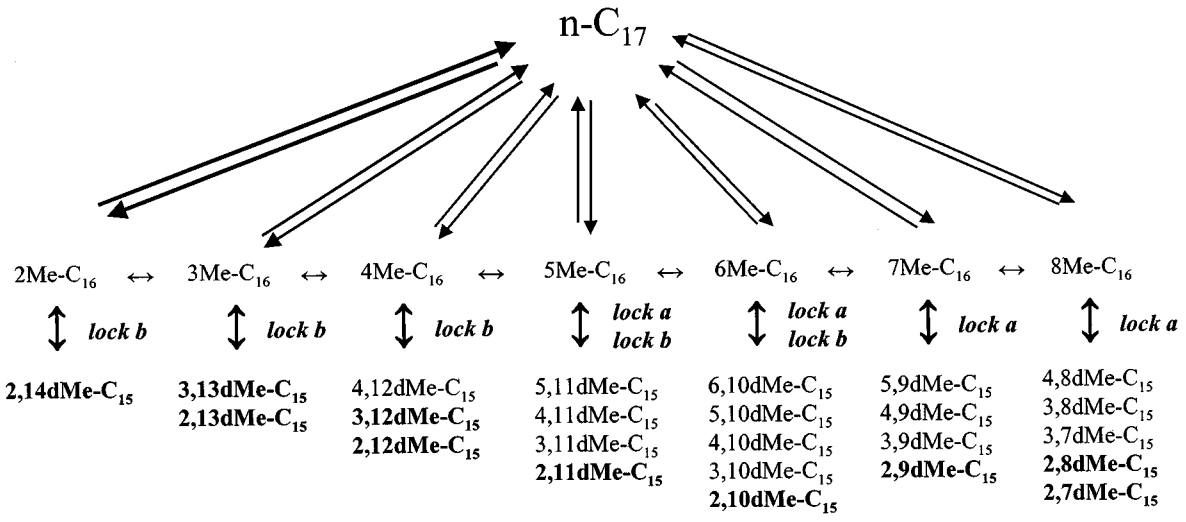

FIG. 7. Reaction network of *n*–C_{17} methyl branching on Pt/H–ZSM-22 catalyst. Isomers in bold characters are the most favored isomers.

3,*n*dMe–C_{x-2} and 4,*n*dMe–C_{x-2} isomers are favored. This evolution reflects the increasing number of positional combinations with methyl groups in other than C_2 positions, respecting the minimum distances between the branchings imposed by the locks.

The formation of dimethylalkanes with symmetric methyl positions revealed special features of the key-lock mechanism. For chains of C_{17} and shorter, the 2,*x*-3dMe–C_{x-2} isomer is an abundant isomer formed in lock a or b out of the 2Me–C_{x-1} isomer. With longer chains, the formation of the 2,*x*-3dMe–C_{x-2} isomer is disfavored. For the long chains, there is insufficient anchoring of the terminally methyl-branched moiety of the molecule in the hole of lock *b*. The anchoring is better when the methyl branching is at C_3 or further positions, explaining the favored formation of 3,*x*-4dMe–C_{x-2}, 4,*x*-5dMe–C_{x-2}, and other symmetric isomers with C_5 or C_6 positions for the methyl groups.

APPENDIX

Chromatograms of Skeletal Isomerization Products

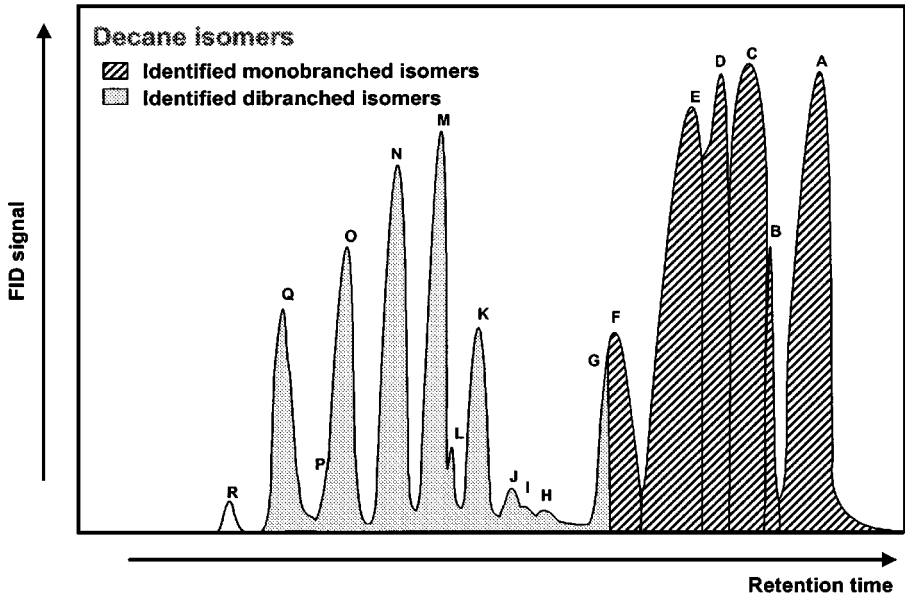

FIG. A1. Chromatogram of decane isomers (*n*-C_{10}). A, 3-methylnonane; B, 3-ethyloctane; C, 2-methylnonane; D, 4-methylnonane; E, 5-methylnonane; F, 4-ethyloctane; G, 2,3-dimethyloctane; H–J, methylethylheptanes; K, 3,6-dimethyloctane; L, 3,5-dimethyloctane; M, 2,6-dimethyloctane; N, 2,7-dimethyloctane; O, 2,5-dimethyloctane, P, 3,4-dimethyloctane; Q, 2,4-dimethyloctane; R, 2,2-dimethyloctane.

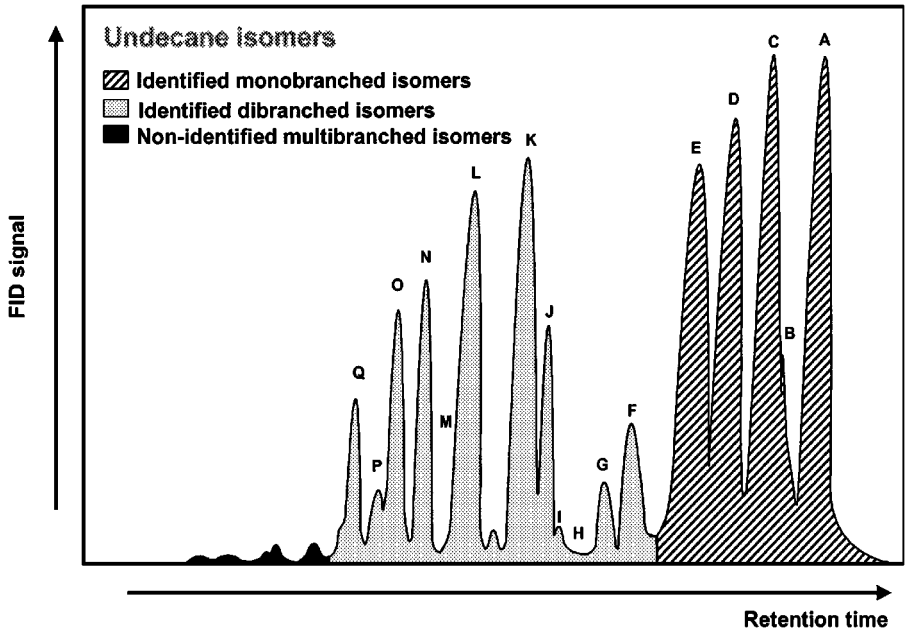

FIG. A2. Chromatogram of undecane isomers (n-C_{11}). A, 3-methyldecane; B, 3-ethylnonane; C, 2-methyldecane; D, 4-methyldecane; E, 5-methyldecane; F–I, methylethyloctanes; J, 3,7-dimethylnonane; K, 2,7-dimethylnonane; L, 2,8-dimethylnonane; M, 3,6-dimethylnonane; N, 2,6-dimethylnonane; O, 2,5-dimethylnonane; P, 3,5-dimethylnonane; Q, 2,4-dimethylnonane.

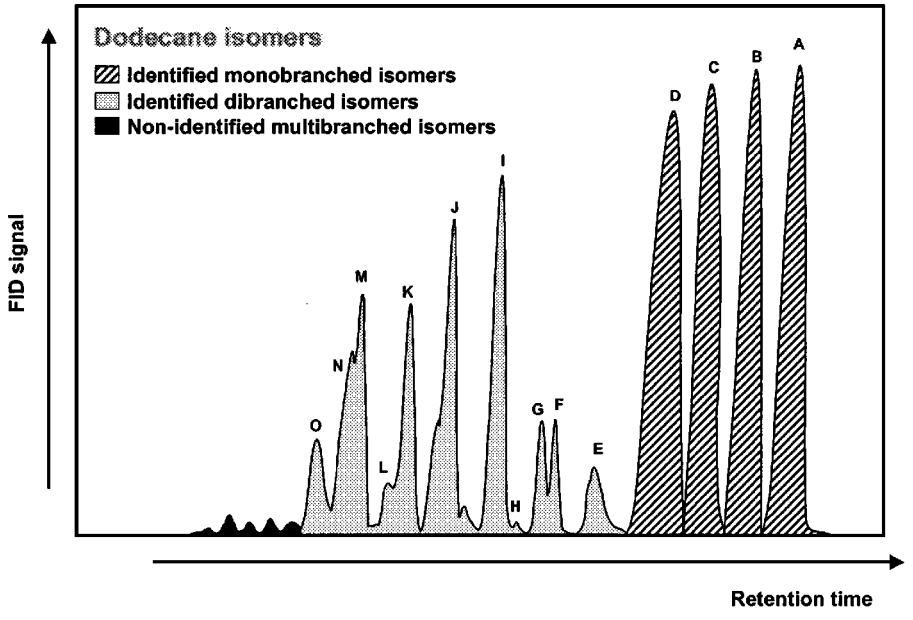

FIG. A3. Chromatogram of dodecane isomers (n-C_{12}). A, 3-methylundecane; B, 2-methylundecane; C, 4-methylundecane; D, 5-methylundecane + 6-methylundecane; E and F, methylethylnonane; G, 3,8-dimethyldecane; H, 3,3-dimethyldecane; I, 2,8-dimethyldecane; J, 2,9-dimethyldecane; K, 2,7-dimethyldecane; L, 3,7-dimethyldecane; M, 2,6-dimethyldecane; N, 2,5-dimethyldecane; O, 2,4-dimethyldecane.

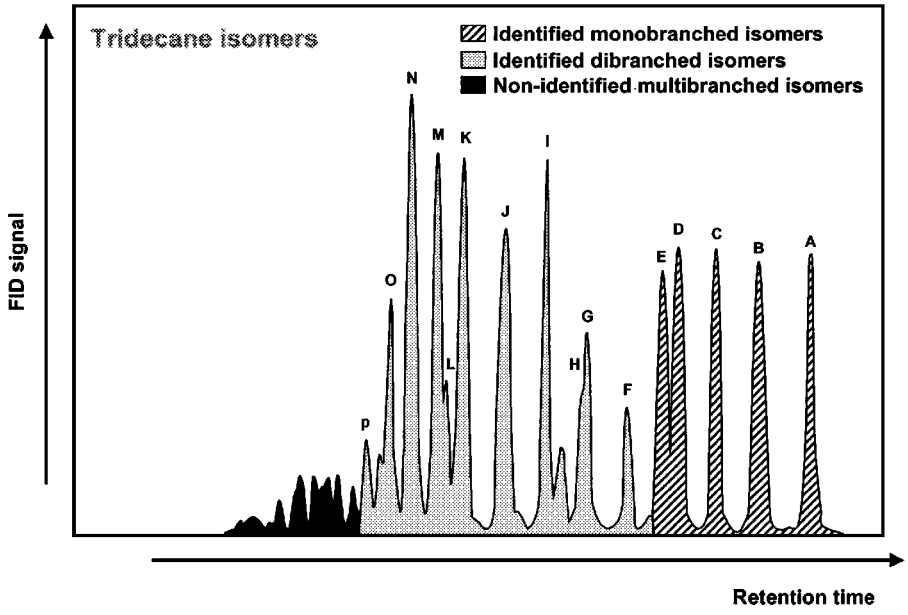

FIG. A4. Chromatogram of tridecane isomers (n-C_{13}). A, 3-methyldodecane; B, 2-methyldodecane; C, 4-methyldodecane; D, 5-methyldodecane; E, 6-methyldodecane; F and G, methylethyldecane; H, 3,9-dimethylundecane; I, 2,9-dimethylundecane; J, 2,10-dimethylundecane; K, 2,8-dimethylundecane + 4,8-dimethylundecane; L, 3,6-dimethylundecane; M, 2,7-dimethylundecane; N, 2,6-dimethylundecane; O, 2,5-dimethylundecane; P, 2,4-dimethylundecane.

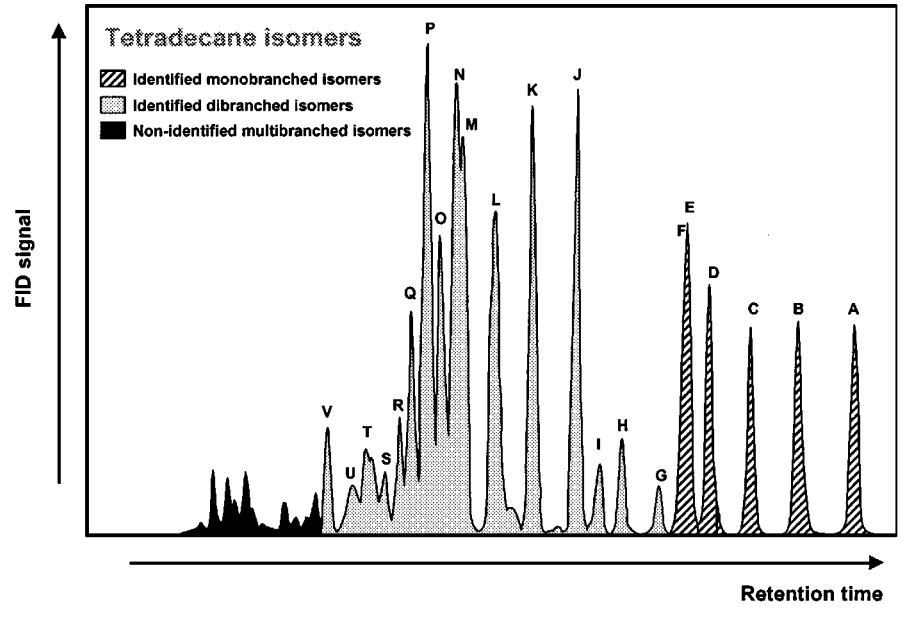

FIG. A5. Chromatogram of tetradecane isomers (n-C_{14}). A, 3-methyltridecane; B, 2-methyltridecane; C, 4-methyltridecane; D, 5-methyltridecane; E, 6-methyltridecane; F, 7-methyltridecane; G and H, methylethylundecane; I, 3,10-dimethyldodecane; J, 2,10-dimethyldodecane; K, 2,11-dimethyldodecane; L, 2,9-dimethyldodecane + 4,9-dimethyldodecane; M, 3,7-dimethyldodecane; N, 2,8-dimethyldodecane + 5,8-dimethyldodecane; O, 2,7-dimethyldodecane; P, 2,6-dimethyldodecane; Q, 2,5-dimethyldodecane; R, 2,4-dimethyldodecane; S, 4,8-dimethyldodecane; T, 4,7-dimethyldodecane; U, 4,6-dimethyldodecane; V, 5,7-dimethyldodecane.

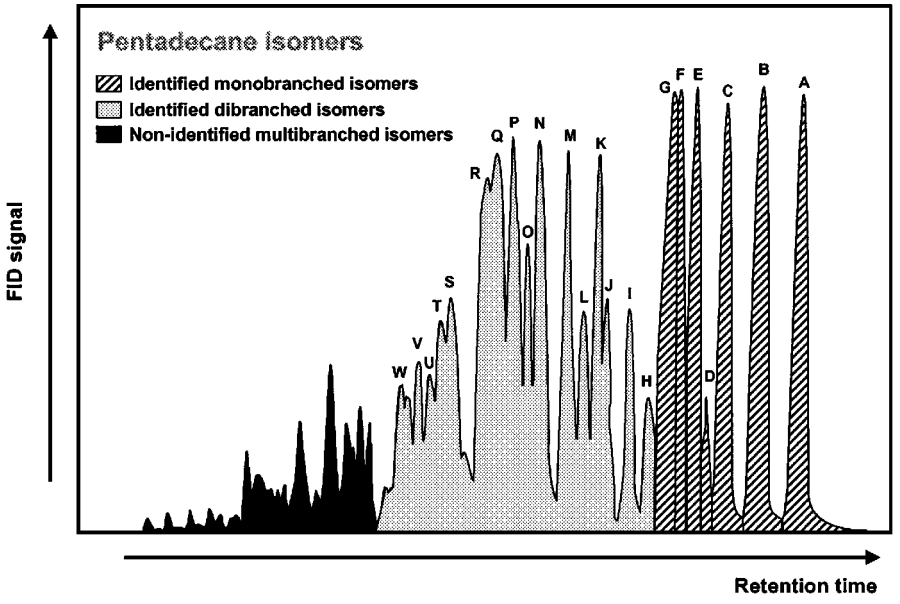

FIG. A6. Chromatogram of pentadecane isomers (n-C_{15}). A, 3-methyltetradecane; B, 2-methyltetradecane; C, 4-methyltetradecane; D, 4-ethyltridecane; E, 5-methyltetradecane; F, 6-methyltetradecane; G, 7-methyltetradecane; H and I, methylethyldodecane; J, 3,11-dimethyltridecane; K, 2,11-dimethyltridecane; L, 3,10-dimethyltridecane; M, 2,12-dimethyltridecane; N, 2,10-dimethyltridecane + 4,10-dimethyltridecane; O, 3,9-dimethyltridecane; P, 2,9-dimethytridecane + 5,9-dimethyltridecane; Q, 6,8-dimethyltridecane + 2,8-dimethyltridecane; R, 2,7-dimethyltridecane + 2,6-dimethyltridecane; S, 4,9-dimethyltridecane; T, 4,8-dimethyltridecane; U, 4,7-dimethyltridecane; V, 5,8-dimethyltridecane; W, 6,7-dimethyltridecane.

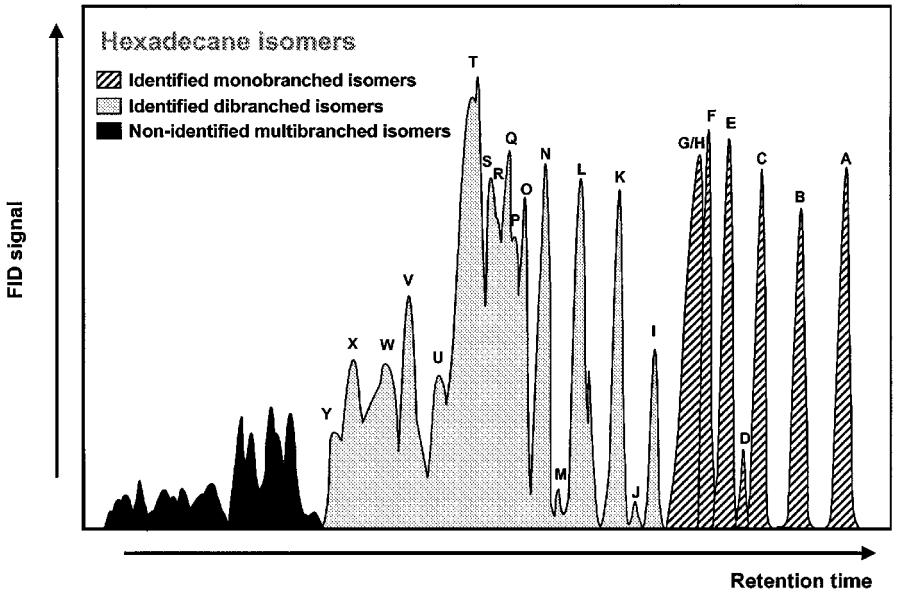

FIG. A7. Chromatogram of hexadecane isomers (n-C_{16}). A, 3-methylpentadecane; B, 2-methylpentadecane; C, 4-methylpentadecane; D, 4-ethyltetradecane; E, 5-methylpentadecane; F, 6-methylpentadecane; G, 7-methylpentadecane; H, 8-methylpentadecane; I and J, methylethyltridecane; K, 2,12-dimethyltetradecane + 3,12-dimethyltetradecane; L, 2,13-dimethyltetradecane + 3,11-dimethyltetradecane; M, methylethyltridecane; N, 2,11-dimethyltetradecane + 4,11-dimethyltetradecane; O, 3,9-dimethyltetradecane; P, 3,8-dimethyltetradecane; Q, 5,10-dimethyltetradecane + 2,10-dimethyltetradecane; R, 3,7-dimethyltetradecane; S, 6,9-dimethyltetradecane; T, 2,9-dimethyltetradecane + 2,8-dimethyltetradecane + 2,7-dimethyltetradecane; U, 4,10-dimethyltetradecane; V, 4,9-dimethyltetradecane + 4,8-dimethyltetradecane + 4,7-dimethyltetradecane; W, 5,9-dimethyltetradecane + 5,8-dimethyltetradecane; X, 6.8-dimethyltetradecane; Y, 6,7-dimethyltetradecane.

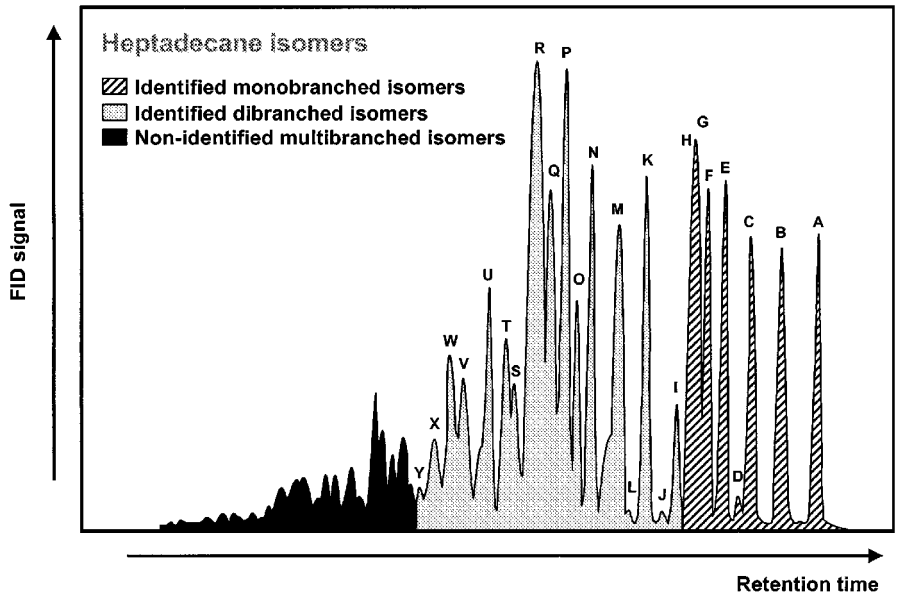

FIG. A8. Chromatogram of heptadecane isomers (n-C_{17}). A, 3-methylhexadecane; B, 2-methylhexadecane; C, 4-methylhexadecane; D, 4-ethylpentadecane; E, 5-methylhexadecane; F, 6-methylhexadecane; G, 7-methylhexadecane; H, 8-methylhexadecane; I and J, methylethyltetradecane; K, 2,13-dimethylpentadecane + 3,13-dimethylpentadecane; L, methylethyltetradecane; M, 2,14-dimethylpentadecane + 3,12-dimethylpentadecane; N, 2,12-dimethylpentadecane + 4,12-dimethylpentadecane; O, 3,10-dimethylpentadecane; P, 5,11-dimethylpentadecane + 2,11-dimethylpentadecane; Q, 6,10-dimethylpentadecane; R, 2,10-dimethylpentadecane + 2,9-dimethylpentadecane + 2,8-dimethylpentadecane + 2,7-dimethylpentadecane; S, 4,10-dimethylpentadecane; T, 4,9-dimethylpentadecane + 4,8-dimethylpentadecane; U, 4,7-dimethylpentadecane; V, 7,9-dimethylpentadecane; W, 5,10-dimethylpentadecane; X, 5,9-dimethylpentadecane + 5,8-dimethylpentadecane; Y, 6,9-dimethylpentadecane + 6,8-dimethylpentadecane.

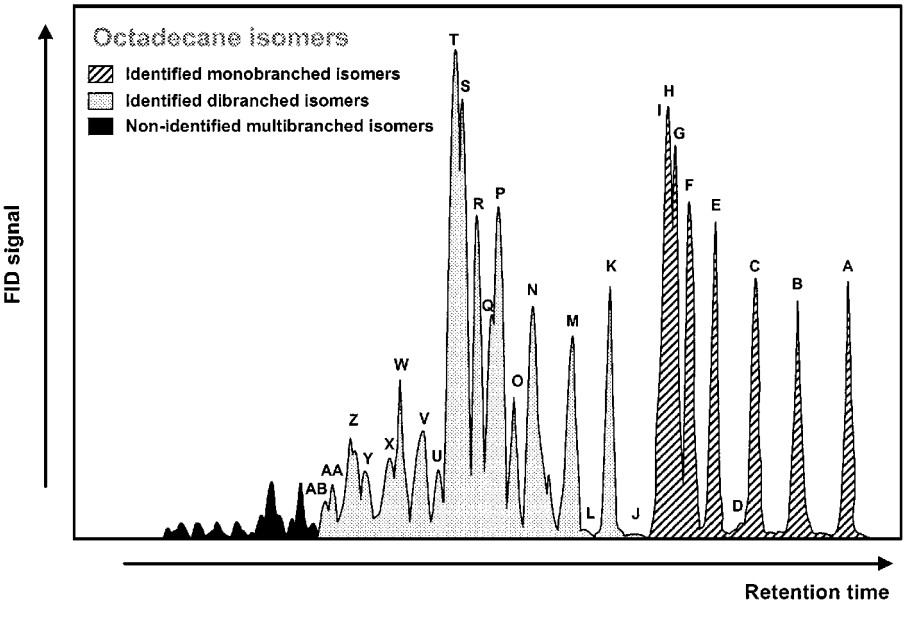

FIG. A9. Chromatogram of octadecane isomers (n-C_{18}). A, 3-methylheptadecane; B, 2-methylheptadecane; C, 4-methylheptadecane; D, 4-ethylhexadecane; E, 5-methylheptadecane; F, 6-methylheptadecane; G, 7-methylheptadecane; H, 8-methylheptadecane; I, 9-methylheptadecane; J, methylethylpentadecane; K, 3,14-dimethylhexadecane; L, methylethylpentadecane; M, 3,13-dimethylhexadecane; N, 4,13-dimethylhexadecane + 2,13-dimethylhexadecane + 3,12-dimethylhexadecane + 3,11-dimethylhexadecane; O, 3,10-dimethylhexadecane; P, 5,12-dimethylhexadecane + 2,12-dimethylhexadecane; Q, 3,9-dimethylhexadecane; R, 6,11-dimethylhexadecane + 2,11-dimethylhexadecane; S, 2,10-dimethylhexadecane; T, 2,9-dimethylhexadecane + 2,8-dimethylhexadecane; U, 4,11-dimethylhexadecane; V, 4,10-dimethylhexadecane + 4,9-dimethylhexadecane; W, 4,8-dimethylhexadecane; X, 7,10-dimethylhexadecane; Y, 5,11-dimethylhexadecane; Z, 5,10-dimethylhexadecane + 5,9-dimethylhexadecane + 5,8-dimethylhexadecane; AA, 6,10-dimethylhexadecane; AB, 6,9-dimethylhexadecane.

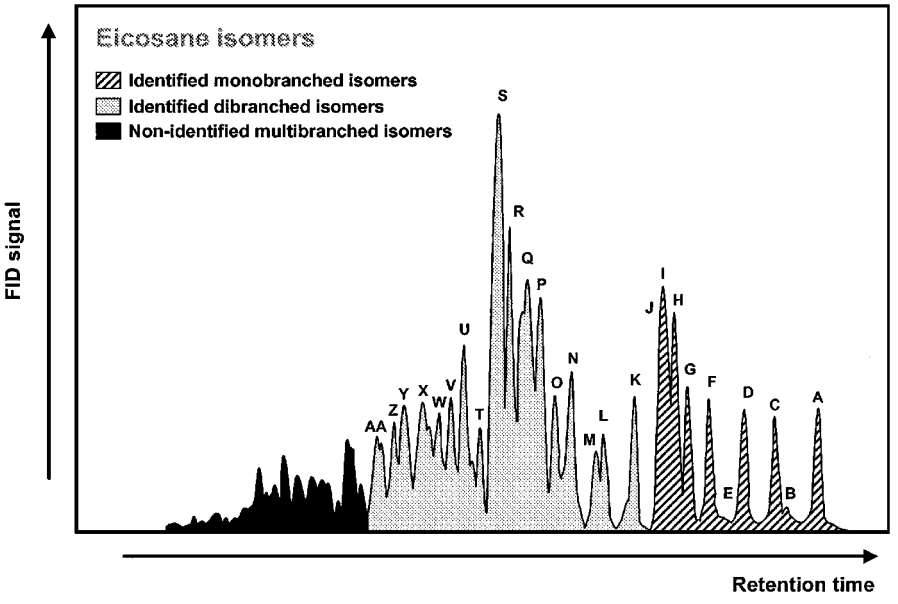

FIG. A10. Chromatogram of eicosane isomers (n-C_{20}). A, 3-methylnonadecane; B, 3-ethyloctadecane; C, 2-methylnonadecane; D, 4-methylnonadecane; E, 4-ethyloctadecane; F, 5-methylnonadecane; G, 6-methylnonadecane; H, 7-methylnonadecane; I, 8-methylnonadecane; J, 9-methylnonadecane; K, 10-methylnonadecane; K, methylethylheptadecane + 3,16-dimethyloctadecane; L, 2,16-dimethyloctadecane + 3,15-dimethyloctadecane; M, 4,15-dimethyloctadecane; N, 3,14-dimethyloctadecane + 2,15-dimethyloctadecane; O, 3,13-dimethyloctadecane; P, 5,14-dimethyloctadecane + 2,14-dimethyloctadecane + 3,12-dimethyloctadecane; Q, 3,10-dimethyloctadecane + 3,9-dimethyloctadecane + 6,13-dimethyloctadecane + 2,13-dimethyloctadecane; R, 2,12-dimethyloctadecane; S, 2,11-dimethyloctadecane + 2,10-dimethyloctadecane + 2,9-dimethyloctadecane + 2,8-dimethyloctadecane; T, 4,13-dimethyloctadecane; U, 4,12-dimethyloctadecane; V, 4,11-dimethyloctadecane; W, 4,10-dimethyloctadecane; X, 4,9-dimethyloctadecane + 4,8-dimethyloctadecane; Y, 5,x-dimethyloctadecane (x = 11 to 13); Z, 5,x-dimethyloctadecane (x = 8 to 10); AA, 6,x-dimethyloctadecane (x = 9 to 12).

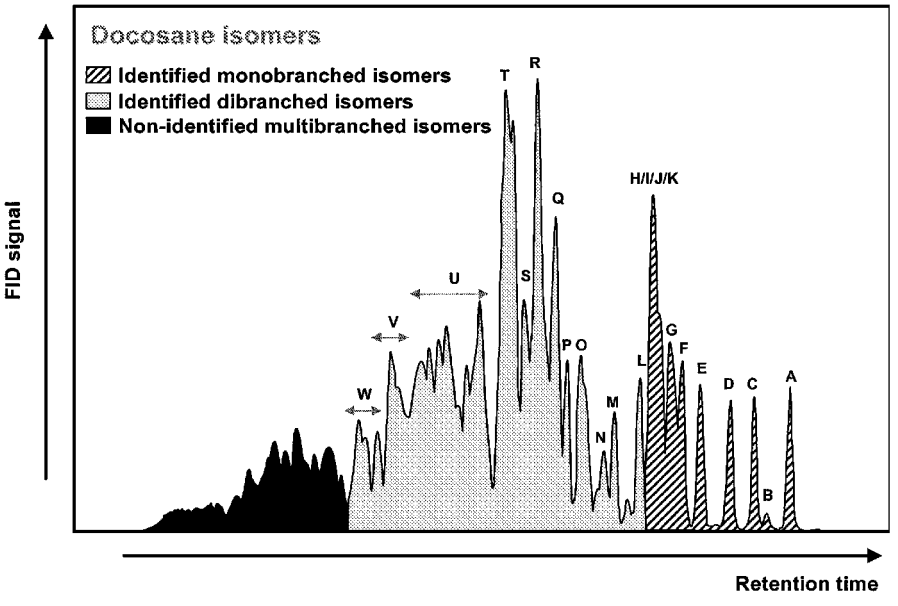

FIG. A11. Chromatogram of docosane isomers (n-C_{22}). A, 3-methyluneicosane; B, 3-ethyleicosane; C, 2-methyluneicosane; D, 4-methyluneicosane; E, 5-methyluneicosane; F, 6-methyluneicosane; G, 7-methyluneicosane; H, 8-methyluneicosane; I, 9-methyluneicosane; J, 10-methyluneicosane; K, 11-methyluneicosane; L, 3,18-dimethyleicosane; M, 3,17-dimethyleicosane; N, 4,17-dimethyleicosane; O, 3,16-dimethyleicosane + 4,15-dimethyleicosane; P, 3,15-dimethyleicosane; Q, 5,16-dimethyleicosane + 3,14-dimethyleicosane + 3,13-dimethyleicosane; R, 3,12-dimethyleicosane + 3,11-dimethyleicosane + 3,10-dimethyleicosane + 3,9-dimethyleicosane + 3,8-dimethyleicosane; S, 6,15-dimethyleicosane; T, 2,12-dimethyleicosane + 2,11-dimethyleicosane + 2,10-dimethyleicosane + 2,9-dimethyleicosane + 2,8-dimethyleicosane; U, 4,x-dimethyleicosane (x = 7 to 14); V, 5,x-dimethyleicosane (x = 9 to 14); W, 7,x-dimethyleicosane (x = 10–13).

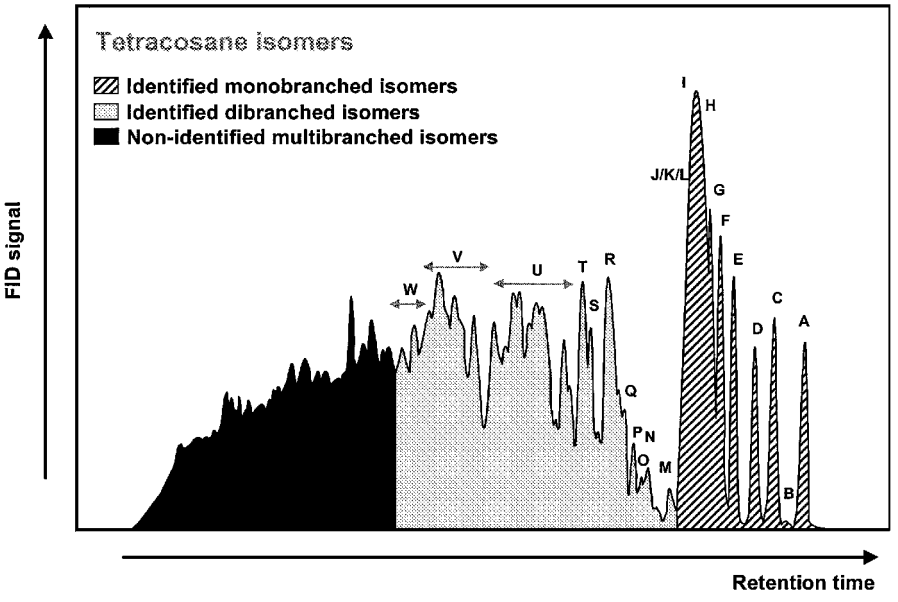

FIG. A12. Chromatogram of tetracosane isomers (n-C_{24}). A, 3-methyltricosane; B, 3-ethyldocosane; C, 2-methyltricosane; D, 4-methyltricosane; E, 5-methyltricosane; F, 6-methyltricosane; G, 7-methyltricosane; H, 8-methyltricosane; I, 9-methyltricosane; J, 10-methyltricosane; K, 11-methyltricosane; L, 12-methyltricosane; M, 3,20-dimethyldocosane + 3,19-dimethyldocosane; N, 4,19-dimethyldocosane; O, 3,18-dimethyldocosane + 2,19-dimethyldocosane + 4,17-dimethyldocosane; P, 3,17-dimethyldocosane; Q, 3,14-dimethyldocosane; R, 3,12-dimethyldocosane 3,11-dimethyldocosane + 3,10-dimethyldocosane + 3,9-dimethyldocosane + 3,8-dimethyldocosane; S, 6,17-dimethyldocosane; T, 2,12-dimethyldocosane + 2,11-dimethyldocosane + 2,10-dimethyldocosane + 2,9-dimethyldocosane + 2,8-dimethyldocosane; U, 4,x-dimethyldocosane ($x = 7$ to 16); V, 5,x-dimethyldocosane ($x = 8$ to 17); W, 6,x-dimethyldocosane ($x = 9$ to 16) + 7,x-dimethyldocosane ($x = 10$ to 15).

ACKNOWLEDGMENTS

This work is part of the Ph.D. of M.C.C., sponsored by Institut Français du Pétrole (Rueil-Malmaison, France). Valuable discussions with E. Benazzi and N. Marchal from IFP were highly appreciated. J.A.M. acknowledges the Belgian government for participation in an IUAP-PAI program and the F.W.O. Vlaanderen for financial support.

REFERENCES

1. Roy, S., Bouchy, C., Pham-Huu, C., Crouzet, C., and Ledoux, M. J., *Stud. Surf. Sci. Catal. C* **130**, 2423 (2000).
2. York, A. P. E., Pham-Huu, C., Del Gallo, P., and Ledoux, M. J., *Catal. Today* **35**, 51 (1997).
3. Miller, S. J., *Stud. Surf. Sci. Catal. C* **84**, 2319 (1994).
4. Miller, S. J., *Microporous Mater.* **2**, 439 (1994).
5. Ernst, S., Kokotailo, G. T., Kumar, R., and Weitkamp, J., "Proceedings, 9th International Congress on Catalysis, Calgary, 1988" (M. J. Phillips and M. Ternan, Eds.), Vol. 1, p. 388. Chem. Institute of Canada, Ottawa, 1988.
6. Ernst, S., Weitkamp, J., Martens, J. A., and Jacobs, P. A., *Appl. Catal.* **48**, 137 (1989).
7. Parton, R., Uytterhoeven, L., Martens, J. A., Jacobs, P. A., and Froment, G. F., *Appl. Catal.* **76**, 131 (1991).
8. Martens, J. A., Souverijns, W., Verrelst, W., Parton, R., Froment, G. F., and Jacobs, P. A., *Angew. Chem. Int. Ed.* **34**, 22 (1995).
9. Claude, M. C., and Martens, J. A., *J. Catal.* **190**, 39 (2000).
10. Mériaudeau, P., Tuan, V. A., Nghiem, T. V., Lai, S. Y., Hung, L. N., and Naccache, C., *J. Catal.* **169**, 55 (1997).
11. Méraudeau, P., Tuan, V. A., Lefebvre, F., Nghiem, V. T., and Naccache, C., *Microporous Mesoporous Mater.* **26**, 161 (1998).
12. Mériaudeau, P., Tuan, V. A., Sapaly, G., Nghiem, V. T., and Naccache, C., *Catal. Today* **49**, 287 (1999).
13. Campelo, J. M., Lafont, F., and Marinas, J. M., *React. Kinet. Catal. Lett.* **62**, 371 (1997).
14. Campelo, J. M., Lafont, F., and Marinas, J. M., *Appl. Catal.* **170**, 139 (1998).
15. Webb, III, E. B., and Grest, G. S., *Catal. Lett.* **56**, 95 (1998).
16. Webb, III, E. B., Grest, G. S., and Mondello, M., *J. Phys. Chem. B* **103**, 4949 (1999).
17. Measen, Th. L., Schenk, M., Vlugt, T. J. H., de Jonge, J. P., and Smit, B., *J. Catal.* **188**, 403 (1999).
18. Schenk, M., Smit, B., Vlugt, T. J. H., and Maesen, T. L. M., *Angew. Chem. Int. Ed.* **113**, 758 (2001).
19. Sastre, G., Chica, A., and Corma, A., *J. Catal.* **195**, 227 (2000).
20. Pieterse, J. A. Z., Veefkind-Reyes, S., Seshan, K., and Lercher, J. A., *J. Phys. Chem. B* **104**, 5715 (2000).
21. Denayer, J. F., Souverijns, W., Jacobs, P. A., Martens, J. A., and Baron, G. V., *J. Phys. Chem. B* **102**, 4588 (1998).
22. Denayer, J. F., Baron, G. V., Vanbutsele, G., Jacobs, P. A., and Martens, J. A., *Chem. Eng. Sci.* **54**, 3553 (1999).
23. Souverijns, W., Martens, J. A., Uytterhoeven, L., Froment, G. F., and Jacobs, P. A., *Stud. Surf. Sci. Catal.* **105**, 1285 (1997).
24. Souverijns, W., Martens, J. A., Froment, G. F., and Jacobs, P. A., *J. Catal.* **174**, 177 (1998).